

## XPS AND IMPEDANCE SPECTROSCOPY OF Gd DOPED CeO<sub>2</sub> SUPERIONIC CERAMICS

T. Šalkus<sup>a</sup>, V. Venckutė<sup>a</sup>, E. Kazakevičius<sup>a</sup>, V. Kazlauskienė<sup>b</sup>, J. Miškinis<sup>b</sup>,  
A. Kežionis<sup>a</sup>, V. Kunigėlis<sup>a</sup>, and A.F. Orliukas<sup>a</sup>

<sup>a</sup> Faculty of Physics, Vilnius University, Saulėtekio 9, LT-10222 Vilnius, Lithuania  
E-mail: tomas.salkus@ff.vu.lt

<sup>b</sup> Institute of Materials Science and Applied Research, Vilnius University, Naugarduko 24, LT-03225 Vilnius, Lithuania

Received 5 June 2009; revised 9 September 2009; accepted 15 September 2009

Ce<sub>0.9</sub>Gd<sub>0.1</sub>O<sub>1.95</sub> (CGO-10) and Ce<sub>0.8</sub>Gd<sub>0.2</sub>O<sub>1.9</sub> (CGO-20) ceramics have been sintered by using commercial powders of Fuel Cell Materials company. The powders of different surface area (BET [m<sup>2</sup>/g]) were used to prepare the ceramics. Elemental compositions of CGO solid electrolytes' surfaces have been investigated in 10<sup>-7</sup> Pa vacuum by X-ray photoelectron spectroscopy and the ratio Ce<sup>4+</sup>/Ce<sup>3+</sup> has been estimated. Electrical parameters of CGO ceramics were investigated in the frequency range from 1 MHz to 1.2 GHz. Temperature-dependant bulk ionic conductivity ( $\sigma_b$ ) was found to follow the Arrhenius law. Ionic conductivity of CGO-10 was higher compared to that of CGO-20. The bulk ionic conductivity of CGO-10 ceramics slightly depended on the grain size of initial powder.

**Keywords:** CeO<sub>2</sub>, ceramics, XPS, ionic conductivity

**PACS:** 61.10.Nz, 66.30.Hs, 81.05.Je, 82.45.Yz

### 1. Introduction

CeO<sub>2</sub> has fluorite-type crystal structure (space group Fm $\bar{3}$ m) in the temperature range from 313 to 1770 K [1]. At high temperatures and low oxygen partial pressures, Ce<sup>4+</sup> in ceria is reduced to Ce<sup>3+</sup> [2]. Therefore ceria is often referred to as CeO<sub>2- $\delta$</sub>  (where  $\delta = [\text{Ce}^{3+}]/2$ ) [2]. Due to relatively low ionic conductivity of pure CeO<sub>2</sub>, a doping of the oxide by different valence metal oxides such as Gd<sub>2</sub>O<sub>3</sub> or Sm<sub>2</sub>O<sub>3</sub> is frequently undertaken. Oxygen vacancies (V<sub>O</sub><sup>••</sup>) being responsible for oxygen ionic transport are created in the Gd<sub>2</sub>O<sub>3</sub> or Sm<sub>2</sub>O<sub>3</sub> doped ceria.

Solid oxide electrolytes with fast V<sub>O</sub><sup>••</sup> transport are used in Solid Oxide Fuel Cells (SOFC). Despite a high ionic conductivity (higher than yttria-stabilized zirconia – YSZ) CGO is not suitable material for SOFC membrane because of its Ce<sup>4+</sup> reduction to Ce<sup>3+</sup> and an uprising electronic conductivity at low oxygen partial pressure (in H<sub>2</sub> atmosphere) [3, 4]. On the other hand, CGO can be prepared as a solid electrolyte and Ni porous composite and so it can be used as an anode material. Composites with CeO<sub>2</sub>-Gd<sub>2</sub>O<sub>3</sub> electrolyte are now intensively investigated [5, 6].

The cubic lattice parameter of Ce<sub>0.9</sub>Gd<sub>0.1</sub>O<sub>1.95</sub>

(CGO-10) is 5.418 Å [7], the density found from X-ray diffraction experiment ( $d_{\text{X-ray}}$ ) is 7.12 g/cm<sup>3</sup> [8], while the lattice parameter of Ce<sub>0.8</sub>Gd<sub>0.2</sub>O<sub>1.9</sub> (CGO-20) is 5.4243(6) Å, with  $d_{\text{X-ray}} = 7.24$  g/cm<sup>3</sup> [2]. Electrical properties of the above-mentioned ceramics have been investigated at frequencies up to 1 MHz [2, 8, 9]. Normally the total conductivity of the ceramics can be found from data in the frequency range up to 1 MHz. To our knowledge there were no impedance spectroscopy experiments performed on CGO in the higher frequency range, from 1 MHz to 1 GHz, where dispersion of electrical properties in the bulk of the ceramics can be observed.

In the present work, CGO-10 and CGO-20 ceramics were sintered from powder with different surface area (BET [m<sup>2</sup>/g]) and studied by scanning electron microscopy (SEM), X-ray photoelectron spectroscopy (XPS), and impedance spectroscopy in the frequency range from 1 MHz to 1.2 GHz.

### 2. Experiment

Powder of CGO-10 with different BET (6.44, 158.03, and 201 m<sup>2</sup>/g) and CGO-20 (BET = 220 m<sup>2</sup>/g) (Fuel Cell Materials, USA) was used for ceramics'

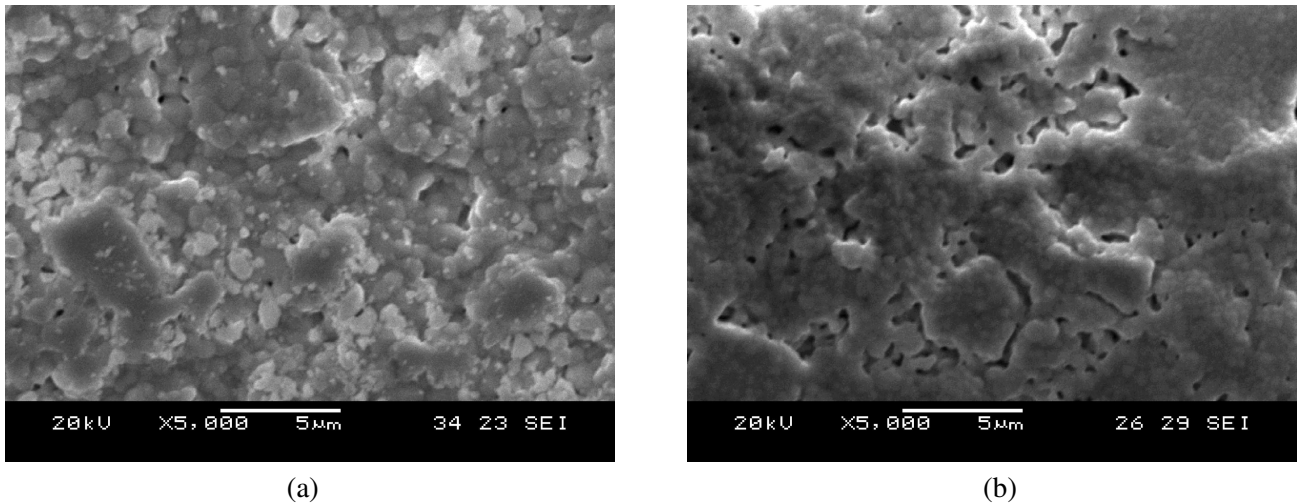


Fig. 1. SEM images of (a) CGO-10 ceramics prepared from powder with  $BET = 6.44 \text{ m}^2/\text{g}$  and (b) CGO-20 ceramics prepared from powder with  $BET = 220 \text{ m}^2/\text{g}$ .

preparation. The powder was pressed at 300 MPa pressure in a 8 mm die. The sintering of the ceramics was performed at 1773 K for 1 h in air. The surfaces of the ceramics were observed by a scanning electron microscope (SEM JSM5600).

Elemental compositions of CGO solid electrolytes' powder and ceramics were investigated in  $10^{-7}$  Pa vacuum by XPS. XPS measurements were recorded by LAS-3000 equipment (RIBER, France) on CGO powder and ceramics using Al  $K\alpha$  ( $h\nu = 1486.6 \text{ eV}$ ) radiation source. The samples were kept inside the XPS high vacuum chamber overnight (without X-ray or electron irradiation) before performing the measurements.

The XPS spectra have been corrected because of the sample charging by referencing binding energy of C 1s 284.6 eV. The spectra were resolved in the Gaussian–Lorentzian components after Shirley background subtraction by XPSPEAK41 software.

Impedance spectrometer based on P4-37 instrument measures the transmission coefficient  $\tilde{T}$  of the sample in a coaxial line in the frequency range from 1 MHz to 1.2 GHz. Impedance of the sample  $\tilde{Z}(f) = Z' - iZ''$ , specific impedance of the material  $\tilde{\rho} = \tilde{Z}S/l$  (where  $S$  is the area of the electrode,  $l$  is the length of the sample), and complex conductivity  $\tilde{\sigma}(f) = \sigma' + i\sigma'' = 1/\tilde{\rho}$  were calculated from  $\tilde{T}$  as described in [10–12]. The measurements of electrical parameters were performed

in the temperature range 450–700 K. The temperature of the sample was measured by a K-type thermocouple.

### 3. Results and discussion

Typical microstructure of the CGO-10 and CGO-20 surfaces is shown in Fig. 1. The experimental densities ( $d$ ) and relative densities ( $d/d_{X\text{-ray}}$ ) of the obtained ceramics are presented in Table 1.

The XPS spectra have been linearly shifted so that the peak of C 1s line corresponded to 284.6 eV because of the sample charging. In Fig. 2 XPS spectra are shown after Shirley background subtraction. The spectrum of Ce 3d can be divided into several components as shown in Fig. 3. Lines marked as 1, 1', 2, 2', 3, 3' can be attributed to  $\text{Ce}^{4+}$  and lines marked as 4, 4', 5, 5' to  $\text{Ce}^{3+}$ . The concentration of Ce(III) is then proportional to the total area of 4, 4', 5, and 5' peaks and the concentration of Ce(IV) is proportional to the total area of 1, 1', 2, 2', 3, and 3' peaks.

The concentration of Ce(III) was calculated in the same way as in [13] according to formula

$$[\text{Ce}^{3+}] \% = \frac{[\text{Ce}^{3+}]}{[\text{Ce}^{3+}] + [\text{Ce}^{4+}]} \cdot 100, \quad (1)$$

Table 1. Experimental densities and electrical properties of CGO-10 and CGO-20 ceramics.

Compound	BET, $\text{m}^2/\text{g}$	$d$ , $\text{g}/\text{cm}^3$	$d/d_{X\text{-ray}}$ , %	$\sigma_b$ , S/m (700 K)	$\Delta E_b$ , eV
CGO-10	6.44	7	98	0.286	0.66
	158.03	6.79	95.4	0.302	0.65
	201	6.87	96.5	0.288	0.66
CGO-20	220	6.86	94.8	0.0702	0.78

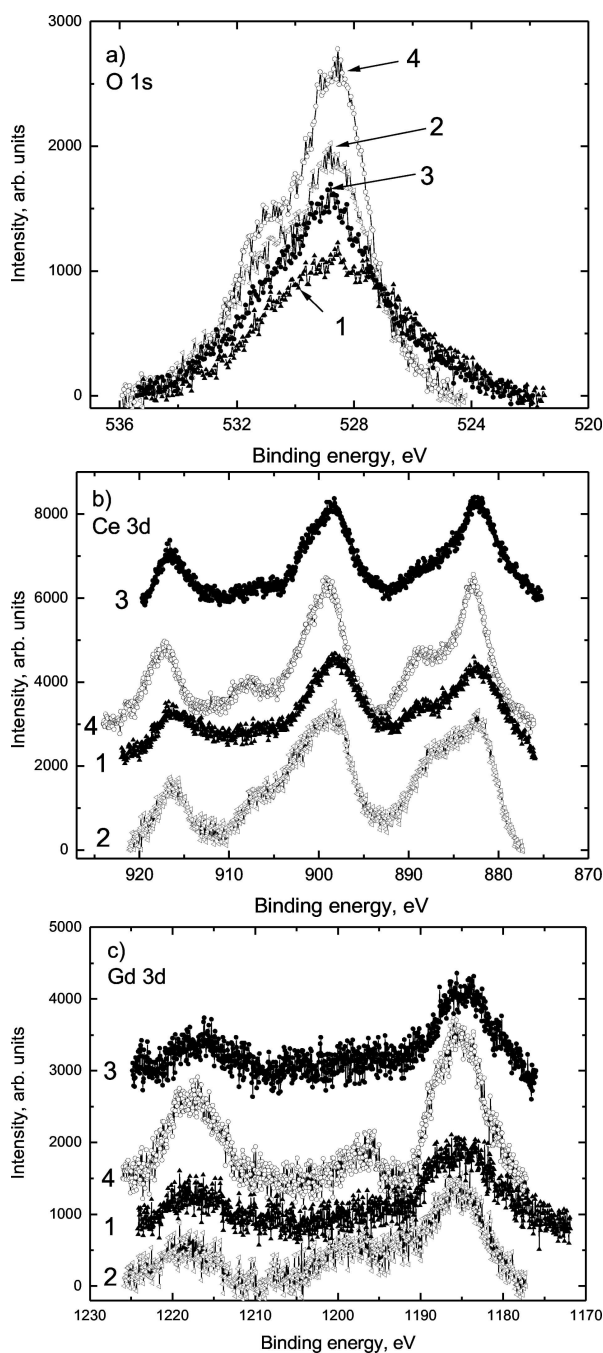


Fig. 2. (a) O 1s, (b) Ce 3d, and (c) Gd 3d XPS spectra of CGO-10 ceramics prepared from powder with BET = 6.44 m<sup>2</sup>/g (1, closed triangles), CGO-10, BET = 158.03 m<sup>2</sup>/g (2, open triangles), CGO-10, BET = 201 m<sup>2</sup>/g (3, closed circles), and CGO-20, BET = 220 m<sup>2</sup>/g (4, open circles).

where [Ce<sup>3+</sup>] and [Ce<sup>4+</sup>] are concentrations of Ce(III) and Ce(IV) respectively. Table 2 shows the amounts of Ce(III) and Ce(IV) in the studied CGO-10 and CGO-20 solid electrolytes. Elemental compositions of the investigated CGO-10 and CGO-20 powder and ceramics have been found from XPS after elimination of carbon and oxygen with O 1s electrons' binding energies

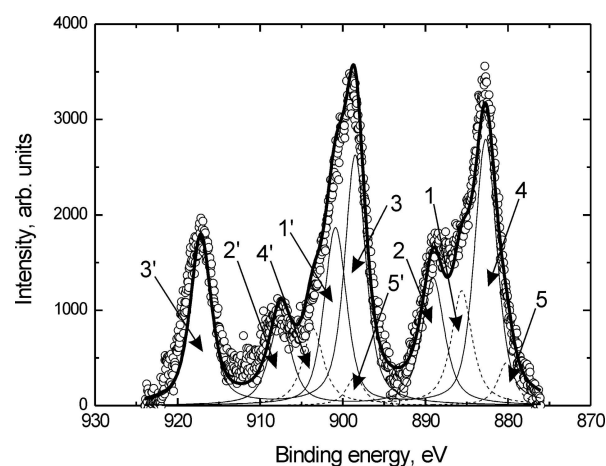


Fig. 3. Ce 3d X-ray photoelectron spectrum of CGO-20 powder. Circles represent experimental data, solid lines have been caused by Ce(IV), dashed lines by Ce(III), bold line is the sum of the peaks.

Table 2. The amounts of Ce(III) and Ce(IV) in CGO-10 and CGO-20 solid electrolytes.

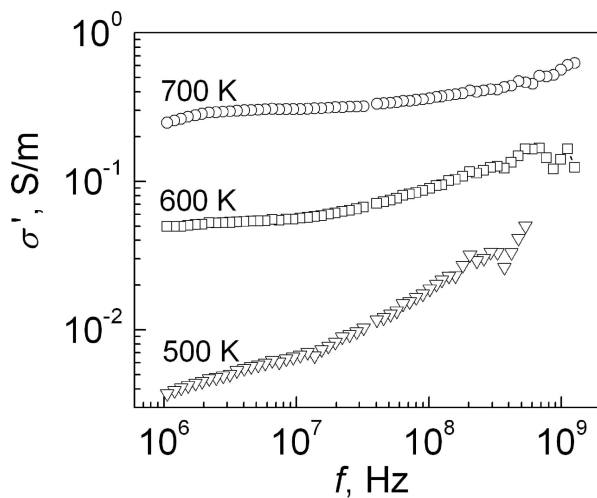
Compound	BET, m <sup>2</sup> /g	Ce(III), atomic %	Ce(IV), atomic %
CGO-10 powder	6.44	27.7	72.3
	158.3	30.7	69.3
CGO-20 powder	201	21.6	78.4
	220	27.5	72.5
CGO-10 ceramics	6.44	19.0	81.0
	201	9.0	91.0

over 531 eV, which can belong to surface contamination. XPS can only yield information from the top several nanometres' surface layer of the sample due to the short inelastic mean free paths of photoelectrons. The electron inelastic mean free paths for Ce 3d and Gd 3d photoelectrons are about 10 Å but for Ce 4d and Gd 4d photoelectrons they are about 30 Å [14]. So, XPS investigations showed a surface composition of powder particles or of ceramic crystallites. Thus we can get some information about the character of composition depth profile by a comparison of quantifications that have been estimated by analysing XPS spectra of Ce and Gd photoelectrons with different mean free path.

The elemental compositions are presented in Table 3 as ratios Gd/Ce and O/(Ce+Gd). These results show that the surfaces of particles (powder) and crystallites (ceramics) are enriched by Gd. The surface enrichment by Gd has also been found in gadolinium doped ceria nanocrystals [15] and Gd doped ceria thin films [16]. The amount of oxygen was found to be close to stoichiometric on the surface of powder particles, but after sintering process the ratio drastically increased and O/(Ce+Gd) > 2.4 has been found on the surface of the

Table 3. Elemental compositions of CGO-10 and CGO-20 solid electrolytes found from XPS (shown as ratios Gd/Ce and O/(Ce+Gd)).

Compound	BET, m <sup>2</sup> /g	Gd/Ce	O/(Ce+Gd)	Gd/Ce	O/(Ce+Gd)
		Ce 3d, Gd 3d electrons used	Ce 3d, Gd 3d electrons used	Ce 4d, Gd 4d electrons used	Ce 4d, Gd 4d electrons used
CGO-10 powder	6.44	0.28	1.82	0.16	1.74
	158.3	0.18	1.94	0.13	1.72
	201	0.15	1.99	0.09	1.8
CGO-20 powder	220	0.23	1.99	0.37	1.89
CGO-10 ceramics	6.44	0.2	2.45	0.15	2.41
CGO-10 ceramics	201	0.31	3.67	0.31	2.81

Fig. 4. Frequency dependences of the real part of conductivity of CGO-10 ceramics prepared from powder with BET = 158.3 m<sup>2</sup>/g and measured at different temperatures.

ceramics. Oxygen partial pressure changes caused not only a reduction of CeO<sub>x</sub> at the surface and in the bulk of crystallites by oxygen diffusion through the oxygen vacancies' net in the crystal lattice [17], but also a formation of the adsorbed species such as O<sub>2</sub><sup>-</sup>, or O<sub>2</sub><sup>=</sup>, or O<sup>=</sup> [18, 19].

The characteristic frequency dependences of the real part of  $\tilde{\sigma}$  of CGO-10 ceramics prepared from powder with BET = 158.03 m<sup>2</sup>/g are shown in Fig. 4. A dispersion region found in  $\sigma'$  spectra was attributed to the fast V<sub>O</sub>•• motion in the bulk of the investigated ceramics. Bulk ionic conductivities ( $\sigma_b$ ) were derived from  $\rho''(\rho')$  plots at different temperatures. As an example the specific impedance in a complex plane of CGO-10 and CGO-20 ceramics measured at 700 K is shown in Fig. 5. The temperature dependences of  $\sigma_b$  of CGO ceramics are shown in Fig. 6. The  $\sigma_b$  is changing with temperature according to the Arrhenius law:

$$\sigma_b = \sigma_0 \exp\left(-\frac{\Delta E_b}{kT}\right), \quad (2)$$

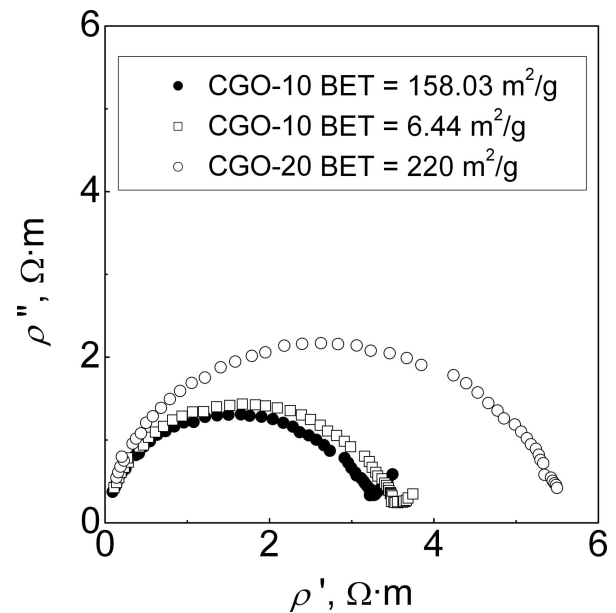


Fig. 5. Complex plane plots of specific impedance at 700 K of CGO-20 and CGO-10 ceramics prepared from powders with different BET.

where  $\sigma_0$  is preexponential factor,  $\Delta E_b$  is activation energy of bulk ionic conductivity,  $k$  is Boltzmann's constant,  $T$  is temperature.

Oxygen ionic bulk conductivity depends on Gd concentration, so a significant increase in conductivity with increasing Gd concentration (5–19%) has been found in high quality thin films [20]. On the other hand, it was found that a plot of activation energy versus dopant concentration showed curve with a minimum in the ceria films [21]. The authors described this minimum in terms of attractive interactions between immobile dopant ions and mobile oxygen vacancies. When the amount of dopant is increased, the oxygen vacancies interact with several dopant ions. The oxygen ion in a saddle-point between sites with interactions with dopant ions will have a lower energy compared to a saddle-point between sites with no interaction with

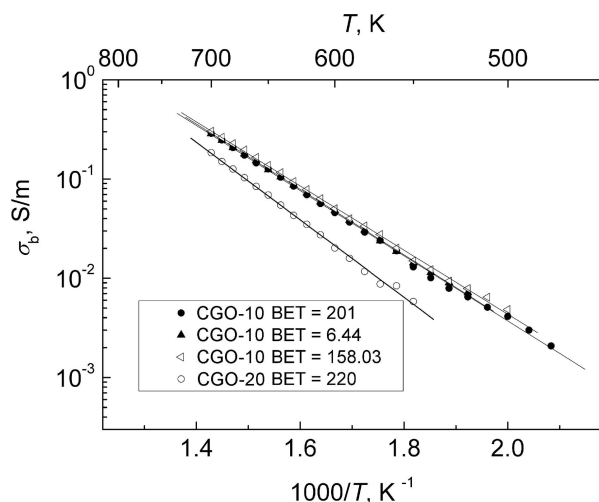


Fig. 6. Temperature dependences of bulk conductivities of CGO-10 ceramics prepared from powders with different BET. BET is shown in  $\text{m}^2/\text{g}$ .

dopant ions. At higher dopant concentrations, deeper traps with dopant ions located next to each other are formed, and the activation energy is higher. The composition associated with the minimum of the activation energy is determined by the interactions of an oxygen vacancy with dopant ions out to a distance of third or fourth nearest neighbours [21].

The comparison of electrical parameters of our studied ceramics is presented in Table 1. It can be seen that the bulk ionic conductivity of CGO-10 ceramics slightly depends on grain size of the initial powder used. Higher conductivity was obtained for ceramics prepared from powder with bigger grain surface area. Ionic conductivity of CGO-20 is lower and activation energy higher compared to CGO-10. Our investigations show some correlation between the activation energy of ionic conductivity (see Table 1) and the amount of dopant (see Table 3) – the activation energy is higher for the compound with higher Gd amount.

#### 4. Conclusions

CGO-10 and CGO-20 ceramics have been sintered. The densities of the obtained ceramics were found to be from 95 to 98% of the theoretical density. It has been shown by XPS that Ce(IV) dominates in the studied CGO solid electrolytes. The relaxation dispersion found in the frequency range  $10^6$ – $1.2 \cdot 10^9$  Hz and temperature range 450–700 K has been attributed to the fast  $V_{\text{O}^{\bullet\bullet}}$  transport in the bulk of the studied CGO ceramics. Bulk ionic conductivities of CGO-10 and CGO-20 varied with temperature according to the Arrhenius law. Higher bulk ionic conductivity ( $\sigma = 0.302$  S/m at

700 K, powder with  $\text{BET} = 158.03 \text{ m}^2/\text{g}$ ) and lower value of activation energy ( $\Delta E_b = 0.65$  eV) were found for the CGO-10 ceramics compared to those of CGO-20.

#### Acknowledgement

This work was supported by the Lithuanian State Science and Studies Foundation.

#### References

- [1] M. Yashima, S. Kobayashi, and T. Yasui, *Solid State Ionics* **177**, 211–215 (2006).
- [2] G. Chiodelli, L. Malavasi, V. Massarotti, P. Mustarelli, and E. Quartarone, *Solid State Ionics* **176**, 1505–1512 (2005).
- [3] T. Matsui, M. Inaba, A. Mineshige, and Z. Ogumi, *Solid State Ionics* **176**, 647–654 (2005).
- [4] S.H. Chan, X.J. Chen, and K.A. Khor, *Solid State Ionics* **158**, 29–43 (2003).
- [5] B. Rösch, H. Tu, A.O. Störmer, A.C. Müller, and U. Stimming, *Solid State Ionics* **175**, 113–117 (2004).
- [6] D. Pérez-Coll, P. Núñez, J.C.C. Abrantes, D.P. Fagg, V.V. Kharton, and J.R. Frade, *Solid State Ionics* **176**, 2799–2805 (2005).
- [7] G. Brauer and H.Z. Gradinger, *Anorg. Allg. Chem.* **276**, 209 (1954).
- [8] C. Xia and M. Liu, *Solid State Ionics* **152–153**, 423–430 (2002).
- [9] M. Dudek, M. Mróz, Ł. Zych, and E. Drożdż-Cieśla, *Mater. Sci. Poland* **26**, 319–330 (2008).
- [10] R. Sobiestianskas, A. Dindune, Z. Kanepe, J. Ronis, A. Kežionis, E. Kazakevičius, and A. Orliukas, *Mater. Sci. Eng. B* **76**, 184–192 (2000).
- [11] W. Bogusz, J.R. Dygas, F. Krok, A. Kezionis, R. Sobiestianskas, E. Kazakevičius, and A. Orliukas, *Phys. Status Solidi A* **183**, 323–330 (2001).
- [12] A.F. Orliukas, A. Kezionis, and E. Kazakevičius, *Solid State Ionics* **176**, 2037–2043 (2005).
- [13] Feng Zhang, Peng Wang, J. Koberstein, S. Khalid, and Siu-Wai Chan, *Surf. Sci.* **563**, 74–82 (2004).
- [14] C.D. Wagner, W.M. Riggs, L.E. Davis, and J.F. Moulder, *Handbook of X-Ray Photoelectron Spectroscopy* (Perkin-Elmer Corporation, Minnesota, 1979).
- [15] E. Rossinyol, E. Pellicer, A. Prim, S. Estradé, J. Arbiol, F. Peiró, A. Cornet, and J.R. Morante, *J. Nanopart. Res.* **10**(2), 369–375 (2008).
- [16] J.L.M. Rupp, T. Drobek, A. Rossi, and L.J. Gauckler, *Chem. Mater.* **19**(5), 1134–1142 (2007).
- [17] N.V. Skorodumova, S.I. Simak, B.I. Lundqvist, I.A. Abrikosov, and B. Johansson, *Phys. Rev. Lett.* **89**(16), 166601 (2002).

- [18] Qing Xu, Duan-ping Huang, Wen Chen, Hao Wang, Bi-tao Wang, and Run-zhang Yuan, *Appl. Surf. Sci.* **228**, 110–114 (2004).
- [19] J.P. Holgado, G. Munuera, J.P. Espinós, and A.R. González-Eliphe, *Appl. Surf. Sci.* **158**, 164–171 (2000).
- [20] D. Bera, S.V.N.T. Kuchibhatla, S. Azad, L. Saraf, C.M. Wang, V. Shutthanandan, P. Nachimuthu, D.E. McCready, M.H. Engelhard, O.A. Marina, D.R. Baer, S. Seal, and S. Thevuthasan, *Thin Solid Films* **516**, 6088–6094 (2008).
- [21] M. Mogensen, N.M. Sammes, and G.A. Tompsett, *Solid State Ionics* **129**, 63–94 (2000).

## CeO<sub>2</sub> SU Gd PRIEDU SUPERJONINIŲ KERAMIKŲ RENTGENO SPINDULIŲ FOTOLEKTRONINIAI IR IMPEDANSINIAI SPEKTRAI

T. Šalkus<sup>a</sup>, V. Venckutė<sup>a</sup>, E. Kazakevičius<sup>a</sup>, V. Kazlauskienė<sup>b</sup>, J. Miškinis<sup>b</sup>, A. Kežionis<sup>a</sup>, V. Kunigėlis<sup>a</sup>, A.F. Orliukas<sup>a</sup>

<sup>a</sup> *Vilniaus universiteto Fizikos fakultetas, Vilnius, Lietuva*

<sup>b</sup> *Vilniaus universiteto Medžiagotyros ir taikomųjų mokslų institutas, Vilnius, Lietuva*

### Santrauka

Tiriamos kepintos CGO-10 ir CGO-20 keramikos. Joms gaminti buvo pasirinkti milteliai su skirtingu grūdelių paviršiaus plotu (BET [m<sup>2</sup>/g]). Elementinė CGO kietųjų elektrolitų sudėtis buvo tiriamiama 10<sup>-7</sup> Pa vakuume Rentgeno spinduliais sužadintų fotoelektronų spektroskopijos metodu, buvo nustatomas Ce<sup>4+</sup>/Ce<sup>3+</sup> santykis bandinių paviršiuje. Elektriniai CGO keramikų parametrai tirti dažniuose nuo 1 MHz iki 1 GHz. Šiame intervale galima išskirti

kristalitinę keramikų laidį ( $\sigma_b$ ). Keičiant temperatūrą,  $\sigma_b$  kinta pagal Arenijaus dėsnį. Kristalitinis CGO-10 keramikų laidis nežymiai priklauso nuo miltelių, iš kurių buvo gaminamos keramikos, grūdelių dydžių. Iš didžiausią paviršiaus plotą turinčių miltelių buvo pagaminta didžiausiu kristaliniu laidžiu pasižyminti CGO-10 keramika, jos kristalinio laidžio aktyvacijos energija  $\Delta E_b = 0,66$  eV. CGO-20 laidis palyginus su CGO-10 yra mažesnis, o aktyvacijos energija didesnė,  $\Delta E_b = 0,78$  eV.